OncoTargets and Therapy

Dovepress
open access to scientific and medical research

Open Access Full Text Article

ORIGINAL RESEARCH

Hypoxic Tumor-Derived Exosomal Circ0048117 Facilitates M2 Macrophage Polarization Acting as miR-140 Sponge in Esophageal Squamous Cell Carcinoma

This article was published in the following Dove Press journal:
OncoTargets and Therapy

Qijue Lu*
Xinyu Wang*
Ji Zhu*
Xiang Fei
Hezhong Chen
Chunguang Li

Department of Thoracic Surgery, Changhai Hospital, The Second Military Medical University, Shanghai, People's Republic of China

*These authors contributed equally to this work

Introduction: Hypoxia and tumor-associated macrophage (TAM) are key regulators in remodeling the microenvironment of esophageal squamous cell carcinoma (ESCC). Hypoxia could stimulate tumor cells to secrete more exosomes and activate TAMs to M2 type. Here, we investigated the function and the underlying mechanism of tumor-derived exosomal hsa-circ-0048117 in TAM polarization in ESCC. Collectively, these data indicate that PC cells generate miR-301a-3p-rich exosomes in a hypoxic microenvironment, which then polarize macrophages to promote malignant behaviors of PC cells.

Methods: Transmission electron microscopy (TEM) and nanoparticle tracking analysis (NTA) were used to analyze the physical characteristics of exosomes. High-throughput sequencing and bioinformatic analysis were performed to screen the potential exosomal circRNA. FISH, Ago2 RIP, pull-down and dual-luciferase reporter assay were conducted to figure out the correlation among hsa-circ-0048117, miR-140 and toll-like receptor 4 (TLR4). Flow cytometry and Western blot were used to evaluate their joint effect in macrophages polarization. Then, the invasion and migration ability were evaluated by transwell experiment. At last, serum exo-hsa-circ-0048117 in ESCC patients was compared and the correlation between its expression and T stage, N stage and TNM grades was analyzed.

Results: Hsa-circ-0048117 was significantly upregulated and enriched in exosomes secreted by hypoxia pre-challenged tumor cells and contributed to M2 macrophage polarization. Hsa-circ-0048117 depletion in macrophage led to inhibition of M2 polarization while restoration of hsa-circ-0048117 could rescue the process. Moreover, hsa-circ-0048117 could act as sponge of miR-140 by competing with TLR4 to facilitate the M2 macrophage polarization. Exo-hsa-circ-0048117 could be transmitted to macrophages to promote M2 polarization and M2 macrophages could enhance the ability of invasion and migration of tumor cells by secreting Arg1, IL-10 and TGF-β. Higher serum exo-hsa-circ-0048117 predicted an advanced T and N stage and positively correlated with TNM grade.

Conclusion: Our findings indicated that ESCC cells generate hsa-circ-0048117-rich exosomes in a hypoxic microenvironment; hsa-circ-0048117 was believed to promote M2 macrophage polarization which favors the malignant behaviors of ESCC cells. These results reminded us that exosomal hsa-circ-0048117 may play a key role in remodeling the microenvironment and modulating progression in ESCC.

Keywords: esophageal squamous cell carcinoma, hypoxia, tumor-associated macrophage, exosomes, hsa-circ-0048117

Correspondence: Chunguang Li
Department of Thoracic Surgery, Changhai Hospital, The Second Military Medical University, No. 168 Changhai Road, Shanghai 200433, People's Republic of China
Tel +86 2131161764
Email dr_lichunguang@sina.com

submit your manuscript | www.dovepress.com
DovePress
http://doi.org/10.2147/OTT.S284192

Background

The oncogenesis and progression of esophageal squamous cell carcinoma (ESCC) is a comprehensive process related to multiple factors, multiple genetic changes and multiple stages of development.[1,2] Tumor microenvironment which includes various tissue cells, inflammatory cells, lymphatic vessels, blood vessels that contribute to tumor growth and metastasis.[3,4] As one of the most important known factors of tumor microenvironment, hypoxia was found to be indispensable in the progression of various malignant tumors.[5] A variety of hypoxic related genes take part in the proliferation, differentiation, invasion and migration of esophageal squamous carcinoma cells through different signaling pathways.[6,7] Hypoxia in malignant tumors such as ovarian cancer, colorectal cancer and pancreatic cancer can promote the development of malignant tumors by affecting the polarization of tumor-associated macrophages (TAMs).[8–10]

Exosomes are widely found in various body fluids such as blood, urine, saliva, cerebrospinal fluid, and breast milk, consisting of mRNA, microRNA, lncRNA, circRNA, DNA fragments, and proteins.[11,12] Tumor cells secrete exosomes containing non-coding RNA and proteins with special functions, which could regulate tumor cell proliferation, apoptosis, invasion and migration.[13–15] A previous study demonstrated tumor cells could produce more exosomes under hypoxia.[16] Circular RNAs are a class of non-coding RNAs that are widely present in eukaryotic organisms and do not contain a 5‘ end cap and a 3′ end Poly tail.[17] They are continuous closed loop structures formed by covalent bonds.[18] Circular RNA was found to function as a competitive endogenous RNA (ceRNA), which can be combined with a specific miRNA to play the role of miRNA “sponge”.[19] Through high-throughput second-generation sequencing and bioinformatics analysis, it has been confirmed that many circular RNAs were involved in the oncogenesis and progression of ESCC,[20] and participating in the regulation of tumor cell proliferation, differentiation, invasion and migration, and formation of the tumor microenvironment.[21,22] Studies have found that the expression abundance of circular RNA in exosomes is significantly higher than that in the producer cells,[23] so we targeted exo-circular RNA, together with bioinformatics analysis, molecular biology and cell function experiments, studied its effect in ESCC and hope to provide a new sight about fundamental research of ESCC.

In this study, we demonstrated that hypoxia promoted ESCC cells to generate more hsa-circ-0048117-riched exosomes, which could induce TAMs differentiate towards M2 type via miR-140/toll-like receptor 4 (TLR4) pathway. M2 macrophages could enhance the invasion and migration ability of ESCC cells. Thus, our results implied that hsa-circ-0048117 could act as a target for exosome mediated tumor immune regulation in ESCC.

Materials and Methods

Blood Samples and Ethical Statement

2 mL of peripheral blood from 62 patients was collected between January and December 2018 at the Thoracic Surgery department, Changhai Hospital. The inclusion criteria: preoperative gastroscopy biopsy pathology was ESCC; no anti-tumor treatment was performed before surgery; no other systemic malignant tumors were combined. Exclusion criteria: pathologically suggestive of adenocarcinoma, compound squamous cell carcinoma including adenosquamous cell carcinoma, small cell squamous cell carcinoma, carcinosarcoma, sarcomatoid carcinoma, etc; accompanied by a second primary cancer; tumor metabolic imaging before treatment suggested that there is distant metastasis; those with other organ dysfunction could not tolerate surgery. The blood of 17 healthy adult volunteers was obtained as control. The clinicpathological features of every patient were obtained from medical records. The study was approved by the Ethics Committee of Changhai Hospital, the Second Military Medical University and adhered to the Declaration of Helsinki. The signed informed consents of all patients and healthy volunteers were obtained prior to the initiation.

Cell Culture and Hypoxia Treatment

ESCC cell line Eca-109, TE-1 and human-derived monocyte macrophage THP-1 were purchased from the Chinese Academy of Sciences (Shanghai, China). Both the cell lines were authenticated by short tandem repeat DNA fingerprinting. Eca-109 cells were cultivated in Dulbecco’s Modified Eagle Medium (DMEM) containing 10% exosome-depleted fetal bovine serum (Life Technologies, USA) and 1% penicillin-streptomycin solution. THP-1 cells were maintained in RPMI-1640 medium consisting of 10% fetal bovine serum (FBS) and 1% penicillin-streptomycin solution. 100 ng/mL Phorbol-12-myristate -13-acetate (PMA, Sigma, USA) was added into medium

for 24–48 hours to induce THP-1 cells (1×10^6) to differentiate into macrophages. Eca-109 cells were classified into 4 groups, 12 hours in hypoxia (12H), 12 hours in normoxia (12N), 24 hours in hypoxia (24H) and 24 hours in normoxia (24N), cells were cultured in a normoxic mode (20% O_2 and 5% CO_2) and hypoxia mode (1% O_2 and 5% CO_2 balanced with N_2) in a 3-gas incubator.

Exosome Isolation, Labeling and Tracking

10 mL supernatant was collected when the confluence of cells reached 80–90% and 2 mL whole blood was drained from volunteers and patients before surgery. exoEasy Maxi Kit (Qiagen, Germany) was applied to isolate and enrich exosomes from medium and serum according to the manufacturer's instructions. Celltracker CM-DiI (Yeasen Bio, China) was used to label exosomes, exosomes were resuspended in sterilized PBS and incubated with 5 μmol/L DiI for 10 min. DiI-exosomes were then washed in PBS 3 times to remove free DiI and other impurities. The result was imaged by laser scanning confocal microscope (Leica Microsystems, Germany). Then, approximately 1×10^8 labeled exosomes were added to the macrophages medium for exosomes uptake studies. Cells were observed under fluorescence microscopy after incubation at 37 °C for 30 min, 2 hours and 12 hours. According to the protocol, 5×10^8 exosomes were used for extraction of exosomal RNA and 1×10^8 exosomes were used for in vitro experimentation with exosomes stimulation.

Transmission Electron Microscope

Exosomes were melted and mixed with an equal amount of 4% paraformaldehyde. 5 ul mixture was added to the copper mesh with a formvar-carbon membrane and washed the membrane with 100 ul sterilized PBS. The copper mesh was placed into 50 ul 1% glutaraldehyde for 5 min at room temperature and then washed with 100 ul ddH_2O. The copper mesh was transferred to 50 ul uranyl oxalate and 50 ul pre-cooled methylcellulose for 5 min and 10 min, respectively. Finally, dry the copper mesh in air for 5–10 min and place it under the JEM1230 transmission electron microscope (JEOL, Japan) and take an electron microscope picture at 80 kV.

Nanoparticle Tracking Analysis

ZetaView PMX 110 (Particle Metrix, Meerbusch, Germany) and the supplementary software ZetaView 8.04.02 were used to record and analyze exosome particle size and concentration. Isolated exosome samples were resuspended with sterilized PBS to make an exosome suspension and inject it into the channel. Record the number of particles counted in the field of view. Generally, the number of cycles is defined as 15 and the test position is 11. Finally set the video resolution and start measuring.

Isolation of RNA and qRT-PCR Analysis

TRIzol reagent (Thermo, USA) was used to isolate cellular RNA and miRNeasy Mini Kit (Qiagen, Germany) was applied to extract total RNA of approximately 5×10^8 exosomes secreted by Eca-109 cells under normoxia and hypoxia treatment. For RNase R digestion, 2 μg of total RNA was incubated for 30 min at 37 °C with or without RNase R (3 U/μg) (Epicentre Technologies, USA) to remove non-circular RNAs. First-strand cDNA was produced with PrimeScript RT Reagent Kit with gDNA Eraser (TaKaRa, Japan) and miRNA reverse transcription was conducted using a Mir-X miRNA qRT-PCR SYBR Kit (Clontech, Japan). Real-time PCR was performed on Roche LightCycler480 (Roche, Switzerland) using the PrimeScript RT Reagent Kit and SYBR Premix Ex Taq (TaKaRa, Japan) with the proper reaction procedures following the manufacturer's instructions. Agarose gel electrophoresis was performed using the products of PCR to detect target circRNA. The primer information used in the research was offered in Table S1.

Microarray Analysis

We use NanoDrop ND-2000 (Thermo Scientific) to quantify RNA and Agilent Bioanalyzer 2100 (Agilent Technologies) to evaluate the integrity of the RNA. sample labeling, microarray hybridization and cleaning were conducted according to the standard procedure. cDNA was harvested after reverse transcription and was synthesized into cRNA and labeled with cyanine-3-CTP. The labeled cRNA was hybridized with the chip, and the original image was obtained with an Agilent Scanner G2505C (Agilent Technologies) after elution. We used the Feature Extraction software (10.7.1.1) to process the original image and obtained the original data. To begin with, the raw data was normalized with the quantile algorithm. The probes that at least 1 condition out of 2 conditions have flags in "P" were chosen for further data analysis. Differentially expressed genes or lncRNAs were then identified through fold change. The threshold set for up- and down-regulated genes was a fold change ≥ 2.0. Afterwards, GO analysis and KEGG analysis were applied to determine the roles of these differentially

expressed mRNAs. Finally, hierarchical clustering was performed to display the distinguishable genes' expression pattern among samples.

Western Blot

30 ug protein was extracted from exosomes or cells and separated by 8% SDS PAGE gel after electrophoresis and then transferred to PVDF membrane via electroblotting. The membrane was blocked with 5% w/v nonfat dry milk for 1 h, anti-CD63 mouse (1:500, ab193349, Abcam, USA), anti-TSG101 mouse (1:500, ab83, Abcam, USA), anti-CD14 rabbit (1:100, ab183322, Abcam, USA), anti-206 rabbit (1:100, ab125028, Abcam, USA), anti-TLR4 rabbit (1:500, ab227383, abcam, USA) and anti-GAPDH mouse (1:500, ab8245, Abcam, USA) were incubated at 4 °C with gentle shaking, overnight. Goat anti-mouse or anti-rabbit antibody was incubated next for 1 h at room temperature. Target proteins were visualized at last with enhanced chemiluminescence reagent.

Oligonucleotide Transfection

Sangon Biotech (Shanghai, China) has synthesized si-hsa-circ-0048117, miR-140 mimics and their corresponding control oligonucleotides. Transfections were conducted using the Lipofectamine 2000 reagent (Invitrogen) according to the protocol of the manufacturer at final concentration of 50 nM of miRNA mimics and siRNAs. The corresponding sequences of oligonucleotides above are as follows: si-hsa-circ-0048117: ATCATGTACACAGATAC ATGAGGCATCATGTACACAGATACAGCA TCATGTA CACAGATACAT, miR-140 mimics: 5′-ACCAUAGGG UAAAACCACU GUU-3′, mimics control: 5′-ACGUGA CACGUUCGGAGAATT-3′.

Plasmids Construction and Stable Transfection

Lentivirus containing hsa-circ-0048117 overexpression sequence which contained circularization processing signal and backsplices sites and corresponding negative control (NC) were synthetized by Genepharma Company (Shanghai, China). Cells were first plated into 6-well plates and grew to a cell confluence of 40–50%. Subsequently, cell infection was performed according to the manufacturer's instructions. Replaced the medium after 6–8 hours and detected the fluorescence expression 48–72 hours after infection. Transfected cells were collected for the following experiments.

The 5637 and T24 cells transfected with pcDNA3.1-

Flow Cytometry

3–5 × 10^5 macrophages after lentivirus infection were trypsinized and counted before detection. Cells were washed with 100 ul sterilized PBS and then resuspended in 100 ul PBS containing 10% FBS after 1 min 1000 rpm centrifugation. Added 1 ug FITC-labeled CD14 antibody and 1 ug PE-labeled CD206 antibody to each tube of cells, incubated at 4 °C for 30 min, and then cells were centrifuged at 1000 rpm for 1 min. Used sterilized PBS to remove free antibody and resuspended cells with 300 ul PBS containing 10% FBS. Cells were passed through Attune NxT flow cytometer (Thermo Fisher, USA) and data were analyzed using the Flowjo software (version 10.0).

Biotin-Coupled Probe Pull-Down Assay

The circRNA pull-down assay was performed following the manufacturer's instructions. Hsa-circ-0048117 biotinylated probe and oligo probe (GenePharma, China) were incubated with magnetic beads (Invitrogen, USA) at room temperature for 2 hours to obtain probe-coated beads. Then approximately 2 × 10^6 macrophages were harvested, lysed, sonicated and then incubated with probe-coated beads at 4 °C overnight. The RNA complexes bound to the beads were eluted and extracted with and the binding miRNAs were analyzed by qRT-PCR assay.

Fluorescence in situ Hybridization (FISH)

Probes targeting hsa-circ-0048117 and miR-140 were designed and synthesized by GenePharma (Shanghai, China). Macrophages were seeded on a cover slip, fixed with 4% paraformaldehyde and penetrated with Triton-X. Mixed the probes and macrophages in incubator at 37 °C overnight for hybridization according to the protocols. DAPI was used for nuclei staining in the dark for 10 min. The signals of probes were detected by the FISH Kit (GenePharma, China) after washing with PBS. Images were acquired by confocal microscope of Leica (Zeiss LSM880 NLO, Leica Microsystems, and Germany). The sequence of probes are as follows: hsa-circ-0048117: 5′-GGTACTT CATGTATCTGTGTACATGATGCC-3′, miR-140: 5′-TACCATAGGGTAAAACCAC TG−3′.

Biotin-Coupled miRNA Capture

Macrophages were transfected with biotinylated miR-140 mimics or miR-scramble (GenePharma, China) according to the standard procedure of Lipofectamine TM 3000

(L3000015, Invitrogen). Macrophages were harvested, washed in cold PBS, and lysed after 24 hours. After being activated and blocked, 50 ul streptavidin-conjugated magnetic beads were incubated with macrophages lysates at 4 °C for 8 h to pull down the biotin-coupled RNA complex. RNeasy Mini Kit was used to extract RNA specifically interacting with miR-140. The abundance of hsa-circ -0048117 was evaluated by qRT-PCR.

Ago2-RNA Immunoprecipitation (Ago2-RIP)

The Ago2-RNA immunoprecipitation (Ago2-RIP) assay was performed according to the manufacturer's guidelines using the Magna RIP RNA-Binding Protein Immunoprecipitation Kit (17–700; Sigma-Aldrich). Anti-argonaute-2 (Ago2) vaccine was the immunoprecipitating antibody (ab32381; Abcam). Macrophages were collected, lysed and sonicated. Added Ago2/IgG antibody into the compounds and incubated at 4 °C overnight. The supernatant was obtained after lysed, washed and centrifugation, TRIzol was used to extract total RNA from the supernatant and qRT-PCR was conducted to assess the abundance of hsa-circ-0048117.

Dual-Luciferase Reporter Assay

Binding sites of hsa-circ-0048117 and miR-140, TLR4 and miR-140 were predicted by the online Target Scan software (targetscan.org). The wild/mutant sequence of hsa-circ-0048117 and TLR4 were synthesized and cloned to pGL3 vector (Promega, Madison, WI). Afterwards, pGL3-hsa-circ-0048117-WT/MUT and pGL3-TLR4-WT/MUT were constructed. The 293T cells were seeded and transfected with pGL3-hsa-circ-0048117-WT/MUT or pGL3-TLR4-WT/MUT and miR-140 mimics or miR-140 mimics negative control according to the instructions of lipofectamine 3000 reagent (Invitrogen). After 48 hours incubation, cells were lysed and the luciferase activity of each group was measured based on directions of the dual luciferase reporter assay kits (Promega, USA).

Cell Invasion and Migration

24-well plates and 8 μm transwell inserts (Corning, USA) were used to evaluate cell invasion and migration ability. For the invasion assay, the insert membranes were coated with matrigel (50 μL/well) (BD, USA) and 5×10^4 Eca-109 cells in 200 ul serum-free medium were added to the upper chamber. 1×10^4 macrophages in 600 ul medium containing 20% FBS and 1×10^8 exosomes were added to the lower chamber. For migration assay, the same procedures were needed except the matrigel coating. After 24 hours of culture, non-migrating or non-invading cells in the upper chamber were removed, cells on the reverse side were fixed with 4% paraformaldehyde for 15 min and stained with 0.1% crystal violet for 30 min. Six visual fields were chosen at random to count the number of cells.

Enzyme-Linked Immunosorbent Assay (ELISA)

The level of Arg-1, IL-10 and TGF-β in supernatant of macrophages were determined by the corresponding enzyme-linked immunosorbent assay (ELISA) kits (Thermo Fisher, USA). The standard curve provided in the kit was used to calculate the cytokine concentrations, expressed as pg/mL based on the conventional sandwich-based ELISA technique. The samples were collected and processed according to the manufacturer's instructions. The absorbance of each well was measured by a spectrophotometer (BioTek, USA) using 450 nm as a detection wave length.

Statistical Analysis

Differences between treated and control groups were analyzed using the Student *t*-test or one-way ANOVA if they followed a normal distribution, otherwise, the Mann–Whitney test was adopted. The correlation between clinical categorical parameters and circ-SETDB1 expression (the median was regarded as the cutoff value) was evaluated by Pearson χ^2 test. All statistical analyses were performed using the SPSS package (version 13.0). A value of $P<0.05$ was considered statistically significant.

Results

Hypoxia Promotes Exosomal Hsa-Circ-0048117 Secretion of ESCC Cells

Exosomes were isolated from the supernatant of identical concentrations of Eca-109 cells. Samples under transmission electron microscopy (TEM) clearly showed a vesicles-like structure with a diameter of about 100 nm (Figure 1A), the median particle size is 116.8 ± 7.6 nm, 117.8 ± 8.5 nm, 112.5 ± 7.9 nm and 114.2 ± 6.6 nm in 12H, 12N, 24H and 24N, respectively, and the percentage of these particle exceeds 98% (Figure 1B and C). The results of the nanoparticle tracking analysis (NTA) showed that the particle concentration was $3.8 \pm 0.7 \times 10^{11}$/mL, $1.4 \pm 0.2 \times 10^{11}$/mL, $1.3 \pm 0.2 \times 10^{12}$/mL and $3.2 \pm 0.3 \times 10^{11}$/mL in 12H, 12N, 24H and

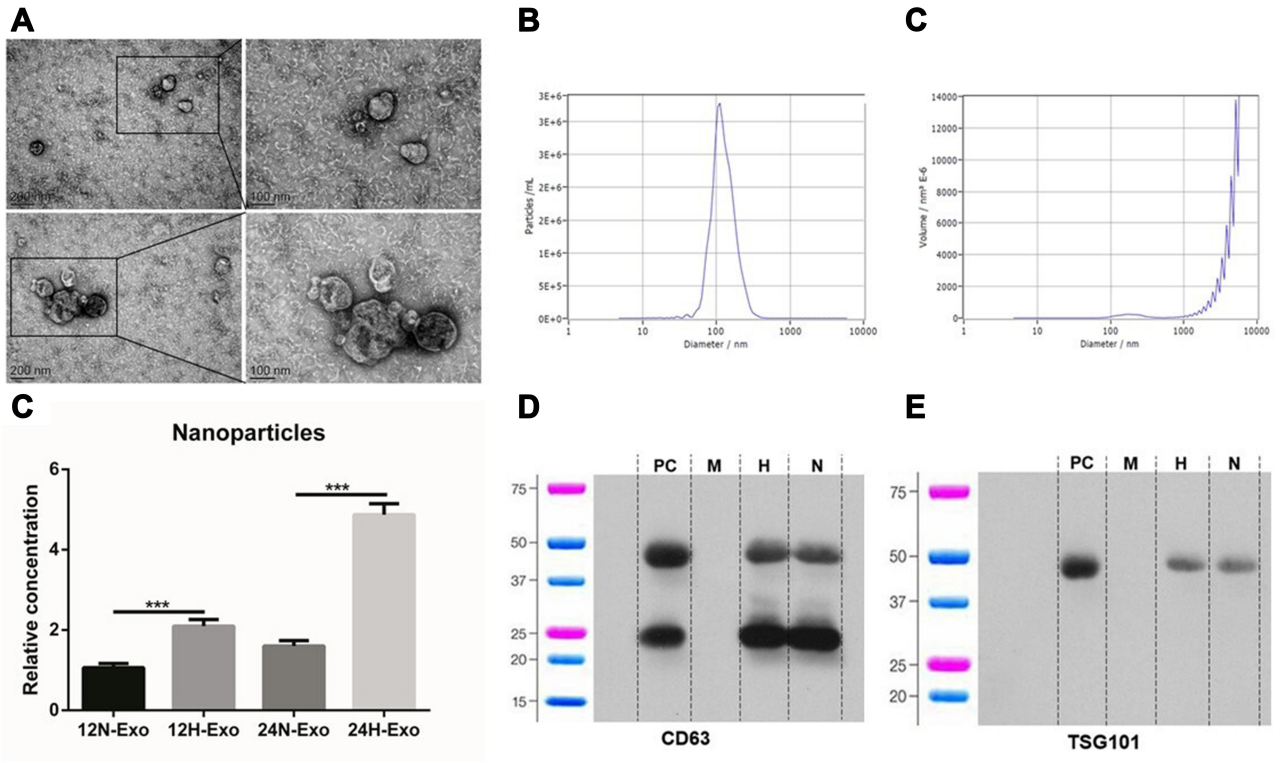

Figure 1 Isolation and identification of exosomes. (**A**) Exosomes isolated from the supernatants of Eca-109 cells under TEM. (**B** and **C**) NTA of exosomes particle concentration and particle size distribution. (**D**) Relative concentration of nanoparticles in 12N, 12H, 24N and 24H (***p<0.01). (**E** and **F**) Western blot analysis for exosomal proteins CD63 and TSG101.

Abbreviations: PC, positive control; M, marker; H, hypoxia; N, normoxia.

24N, respectively, revealing that hypoxia could promote tumor cell to generate more exosomes (Figure 1D). The results of Western blotting showed that the expression of exosome markers CD63 and TSG101 in the samples were strongly expressed (Figure 1E and F).

According to the comprehensive results of microarray analysis (Table 1), box-whisker plot (Figure 2A), scatter plot (Figure 2B), principal component analysis (Figure 2C), clustering analysis (Figure 2E-H) and ceRNA prediction (Figure 2D) were adopted to screen the target circular RNA, we listed top 5 circular RNAs in overall score, as was shown in Table 2. These circRNAs' expressions in exosomes (Figure 3A and B), cells (Figure 3C and D) and serum (Figure 3E and H) were detected by qRT-PCR, the results showed that hsa-circ-0048117 had consistent expression changes and significant differences between hypoxia and normoxia cells, exosomes and serum. Besides, hsa-circ-0048117 in tumor cells and their corresponding exosomes after 24 hours of hypoxia treatment was increased significantly compared with the other three groups (Figure 3F and G). The expression of hsa-circ -0048117 between 12H and 12N also had a significant difference (Figure 3F and G), however, there was no differences found between 12N and 24N (Figure 3F and G). Therefore, hsa-circ-0048117 was decided to be the circular RNA of interest.

Table 1 Differentiated Gene Expression of Microarray Analysis

NO	Test	Cont	mRNA (Regulated)			lncRNA (Regulated)			circRNA (Regulated)		
			Up	Down	Total	Up	Down	Total	Up	Down	Total
1	12H	12N	695	668	1363	1972	1322	3294	526	229	755
2	24H	12H	1365	1025	2390	2426	3005	5431	266	1014	1280
3	24H	24N	345	648	993	793	1221	2014	175	276	451
4	24N	12N	1107	492	1599	2415	1681	4096	299	431	730

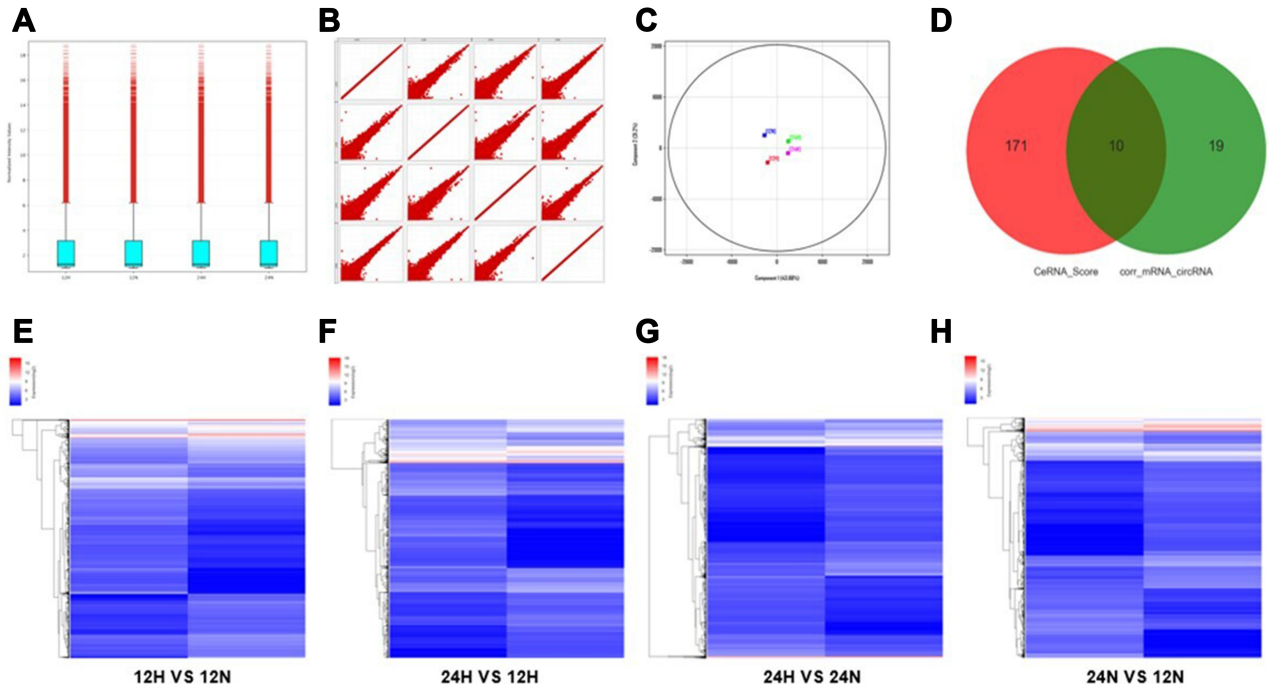

Figure 2 Differential gene screening of microarray and ceRNA analysis. (**A**) Box-whisker plot: minimum, first quartile (25%), median (50%), third quartile (75%) and the maximum value were used to analyze the symmetry and the degree of dispersion of the distribution. (**B**) Scatter plot: evaluate the overall distribution and concentration trend of multiple sets of data. (**C**) Principal component analysis: to examine the distribution of samples to verify the rationality of the experimental design and the uniformity of biological duplicate samples. (**D**) Correlation pairs of circRNA and mRNA were calculated by correlation of expression values. Use this information to further filter the ceRNA predicted by the ceRNA score method. (**E–H**) Clustering: Unsupervised hierarchical clustering of differentially expressed genes and displayed in heatmap. (12H, 12N, 24H and 24N represents 12 hours for hypoxia, 12 hours for normoxia, 24 hours for hypoxia and 24 hours for normoxia, respectively.).

Using Chromas software to analyze the sequencing results, it was found that hsa-circ-0048117 was located in chr19: 964832–968503, consisting of exon6, exon7 and exon8, the spliced sequence length was 644 bp and the splicing site was located at: CAGATA (Figure 4C). PCR product was sequenced to find the corresponding splicing site, suggesting that the cloned sequence was the target sequence, confirming the circular structure of hsa-circ-0048117. The agarose gel results showed that the amplified sequence of hsa-circ-0048117 was 86 bp (Figure 4A). The results of the enzyme tolerance test showed that after RnaseR treatment, the expression of hsa-circ-0048117 did not decrease significantly compared to the internal control GAPDH group (Figure 4B), suggesting that hsa-circ-0048117 was not easily degraded by RnaseR which further testified as to the circular structure.

Hsa-circ-0048117 Could Upregulate TLR4 via Acting as miR-140 Sponge to Promote M2 Macrophage Polarization

According to the CircBase database, the gene symbol of hsa-circ-0048117 was ARID3A which was a transcription factor and was found to be involved in the maturation and differentiation of B lymphocytes, hematopoietic stem cells and macrophages.[24] ARID3A has been implied as acting as a key transcription factor in ESCC,[25] ARID3A expression was inversely correlated with invasion depth, lymph node metastasis, distant metastasis and TNM stage in ESCC.[26]

Table 2 Top 5 Candidate circRNAs in Overall Score

mRNA	circRNA	CeRNA Score	P value	Shared miRNA Number
NM_031407	Hsa-circ-0048117	0.79	1.24E-10	77
NM_015271	Hsa-circ-0028003	0.44	2.74E-06	42
NM_003196	Hsa-circ-0020892	0.18	4.21E-06	38
NM_002153	Hsa-circ-0059462	0.22	0.00271	10
NM_003196	Hsa-circ-0086444	0.29	0.01525	5

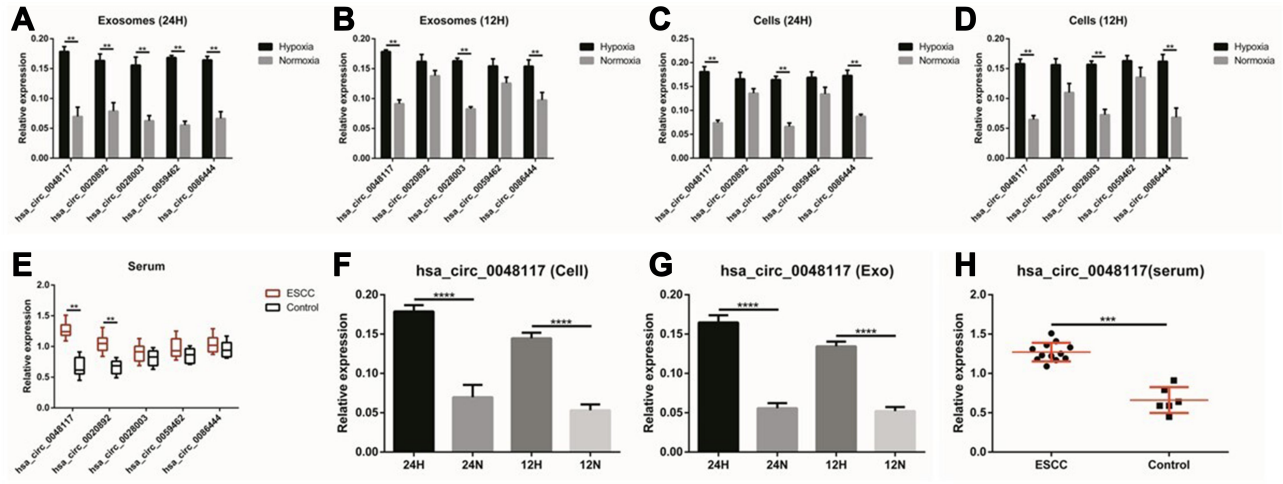

Figure 3 The relative expression of 5 circRNAs in exosomes, cells and serum. (**A** and **B**) The relative expression of the 5 candidate circRNAs in exosomes secreted by Eca-109 cells treated with hypoxia and normoxia after 24 and 12 hours (**p<0.05). (**C** and **D**) The relative expression of the 5 candidate circRNAs in Eca-109 cells treated with hypoxia and normoxia after 24 and 12 hours (**p<0.05). (**E**) The relative expression of the 5 candidate circRNAs in exosomes isolated from serum of 12 ESCC patients (**p<0.05). (**F** and **G**) The relative expression of hsa-circ-0048117 in tumor cells and tumor cells derived exosomes after being treated with hypoxia and normoxia for 12 and 24 hours (****p<0.001). (**H**) The relative expression of hsa-circ-0048117 in exosomes isolated from serum of 12 ESCC patients and 5 healthy volunteers (***p<0.01).

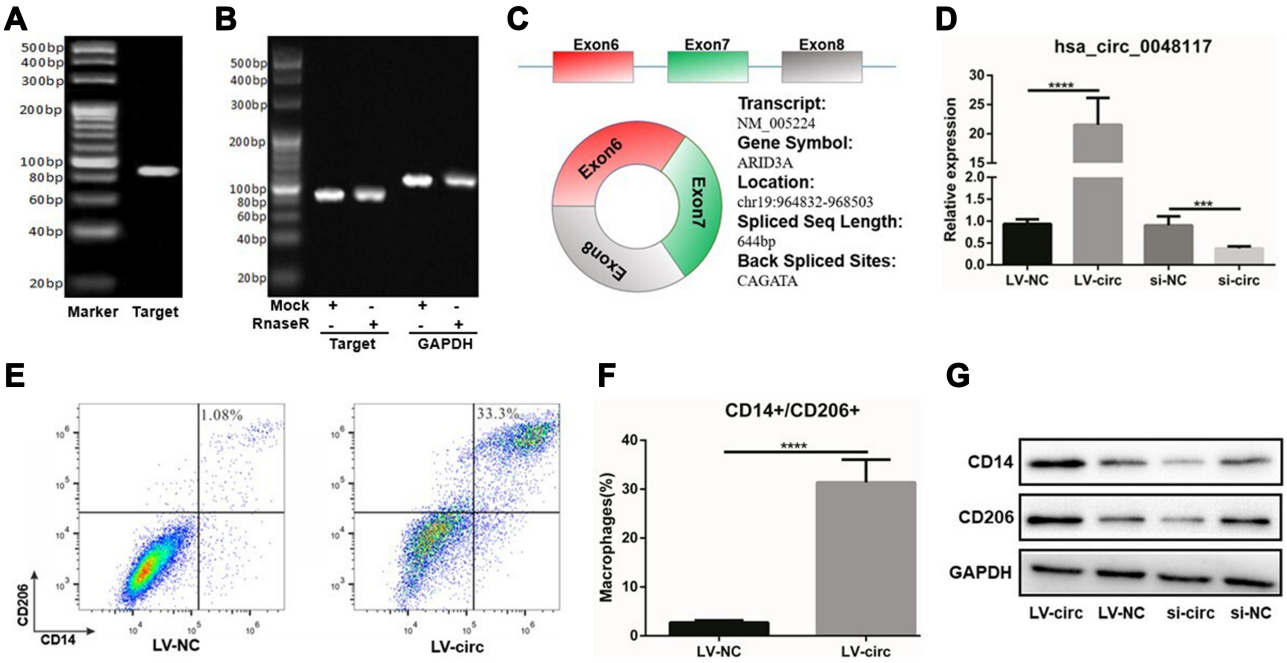

Figure 4 Hsa-circ-0048117 could induce the polarization of M2 macrophages. (**A**) The agarose gel results showed that hsa-circ-0048117 was 86 bp in size. (**B**) The enzyme tolerance test after the RnaseR treatment to testify the circular structure of hsa-circ-0048117. (**C**) The gene information and structure of hsa-circ-0048117: located in chr19: 964832–968503, consisting exon6, exon7 and exon8, the spliced sequence length was 644bp and the splicing site was located at: CAGATA. (**D**) qRT-PCR: to evaluate the transfection efficiency of hsa-circ-0048117 over-expressed and inhibited by lentivirus and siRNA, respectively (***p<0.01). (**E** and **F**) Flow cytometry was used to detect the expression of M2 markers CD14 and CD206 (****p<0.001). (**G**) Western blot was used to examine the expression of CD14 and CD206 after hsa-circ-0048117 was upregulated and downregulated.

Above all, we decided to figure out the relationship of hsa-circ-0048117 and macrophages polarization in ESCC. Human THP-1 monocytes were differentiated into macrophages after 48 hours incubation with PMA, we next designed and synthesized the siRNA and lentivirus vector to silence and magnify the expression of hsa-circ-0048117 in macrophages, respectively. After successful transfection (Figure 4D), Western blot suggested CD14 and CD206 were both increased after hsa-circ-0048117 was overexpressed, and were decreased when hsa-circ-0048117 was

interfered with (Figure 4G). The results of flow cytometry revealed that the percentage of macrophages expressing CD14 and CD206 simultaneously was significantly increased after hsa-circ-0048117 was overexpressed (Figure 4E and F), which demonstrated hsa-circ-0048117 could promote M2 macrophage polarization.

Using AGO2 antibody for RNA immunoprecipitation (RIP) in macrophages, hsa-circ-0048117 was significantly enriched by AGO2 antibody compared to IgG ($p<0.01$) (Figure 5C), suggesting that hsa-circ-0048117 has the potential to be a ceRNA. Circular RNA Interactome and miRanda miRNA target prediction tools were used to screen the miRNAs interacting with hsa-circ-0048117, 31 miRNAs were found possibly binding to hsa-circ-0048117. The top 10 miRNAs were selected based on the context score (Figure 5A), and hsa-circ-0048117 related miRNAs were purified by circRIP. As a result, miR-140 was specifically enriched compared to the other 9 miRNAs and we decided to choose miR-140 as the target miRNA of hsa-circ -0048117 for the following experiments (Figure 5B). The mixed probes of hsa-circ-0048117 and miR-140 were incubated with macrophages for hybridization, FISH detection showed that hsa-circ-0048117 and miR-140 were co-localized in macrophages (Figure 5F). Through a pull-down experiment of the biotin-coupled miR-140 mimic, we observed that hsa-circ-0048117 was significantly enriched in macrophages transfected with miR-140 mimics compared to the control group ($p<0.01$) (Figure 5D). The luciferase reporter experiment showed that miR-140 mimics reduced luciferase activity by at least 50% after binding to hsa-circ -0048117 ($p<0.05$) (Figure 5E). The target site of hsa-circ -0048117 was mutated and the corresponding miRNA was transfected into macrophages, but the luciferase activity did not change significantly ($p>0.05$) (Figure 5E). The predicted binding sequence in miR-140 was GACACCA (Figure 5G). Using siRNA-hsa-circ-0048117 and miR-140 inhibitor to interfere with the expression of hsa-circ-0048117 and miR-140, respectively, and the results of flow cytometry revealed that the percentage of M2 macrophages was significantly increased after miR-140 was silenced and this effect could be neutralized by inhibiting hsa-circ-0048117 simultaneously ($p<0.05$) (Figure 5H and I).

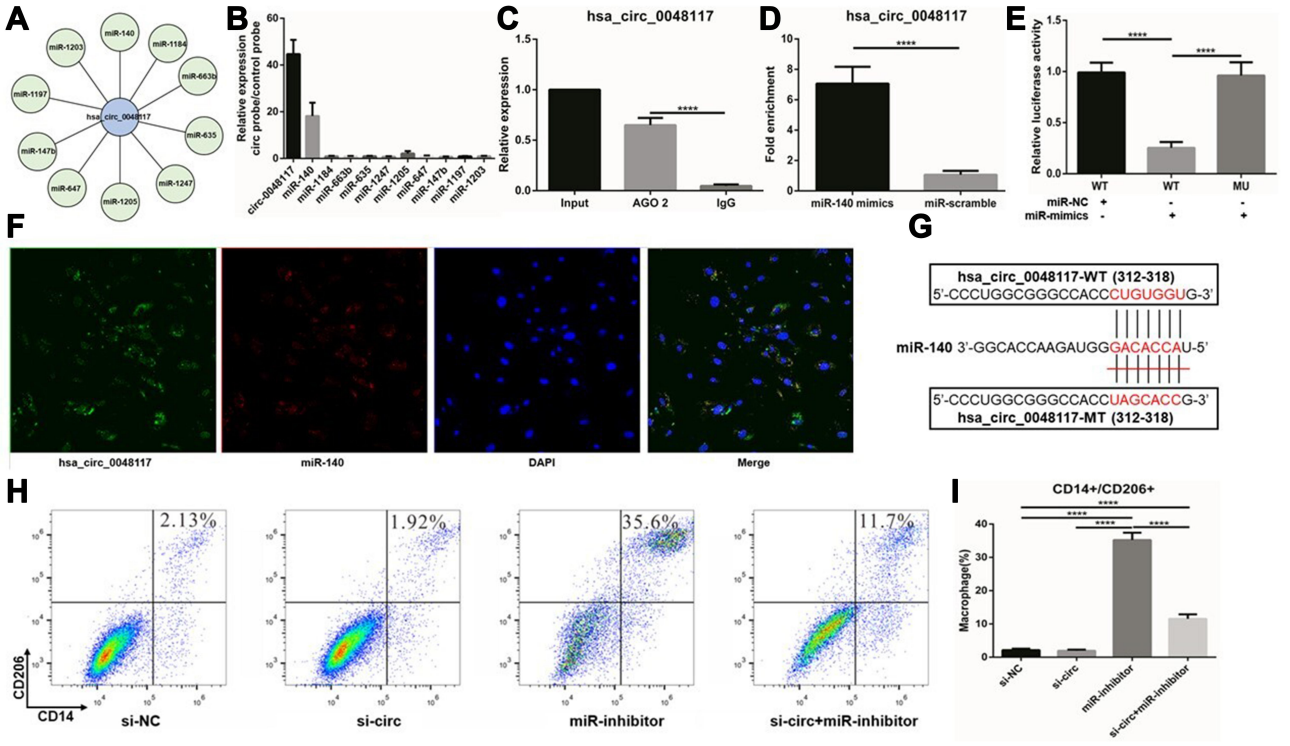

Figure 5 Hsa-circ-0048117 promotes M2 polarization by inhibiting miR-140. (**A**) The 10 candidate miRNAs binding to hsa-circ-0048117 were listed according to RNA Interactome and miRanda miRNA target prediction tools. (**B**) CircRIP was used to purify the hsa-circ-0048117 related miRNAs. (**C**) AGO2 antibody for RNA immunoprecipitation was used to verify hsa-circ-0048117 could be enriched by AGO2 antibody (****p<0.001). (**D**) Pull-down experiment of the biotin-coupled miR-140 mimic was conducted to find hsa-circ-0048117 was significantly enriched in macrophages transfected with miR-140 mimics (****p<0.001). (**E**) The luciferase reporter experiment was applied to detect the luciferase activity after miR-140 mimics binding to hsa-circ-0048117 (****p<0.001). (**F**) FISH detection showed that hsa-circ-0048117 and miR-140 were co-localized in macrophages. (**G**) The predicted binding sequence between miR-140 and hsa-circ-0048117. (**H** and **I**) Flow cytometry was used to detect the M2 markers CD14 and CD206 to check macrophages polarization under the joint effect of miR-140 and hsa-circ-0048117 (****p<0.001).

TLR4 was found to be a potential target of miR-140 according to the miRanda prediction and could participate in the polarization of macrophages as reported in previous studies.[27] TLR4 is a member of the Toll-like receptor family and is widely present on the surface of antigen-presenting cells and macrophages. Studies have confirmed that the activation of TLR4 on the surface of macrophages plays an important role in the differentiation of macrophages. TLR4 is highly expressed in lung cancer TAMs and promotes the conversion of TAMs to M2 type by promoting the oxidative phosphorylation process in mitochondrial metabolism and inhibiting the glycolysis pathway.[28] After treating TAMs with TLR4 agonists, the proportion of M2 macrophages was significantly increased, and co-cultivation of the treated macrophages and tumor cells revealed that macrophages can significantly promote the proliferation of tumor cells.[29] Through cell function experiments, it was found that TLR4 activation in colorectal cancer, liver cancer and lung cancer can promote the transformation of TAMs to M2 type, and enhance the ability of tumor cell growth, invasion and metastasis.[30] Overexpression of hsa-circ-0048117 in macrophages can upregulate the expression of TLR4 (Figure 6D), and the expression of TLR4 was decreased after miR-140 was overexpressed according to the Western blot results (Figure 6C). The luciferase reporter experiment showed that miR-140 mimics significantly reduced luciferase activity after binding to TLR-4 ($p<0.01$), while the luciferase activity did not show a difference when the binding site in TLR-4 was mutated (Figure 6B), the predicted binding site sequence in TLR4 was AACCACU (Figure 6A). These results suggested miR-140 could bind to the 3′-UTR of TLR4 and inhibit its expression. The above experimental results confirmed that hsa-circ-0048117 and TLR4 can competitively bind to miR-140, which are a pair of competitive endogenous RNAs. Hsa-circ-0048117 up-regulates the expression of TLR4 and promoted M2 macrophage polarization through inhibiting miR-140.

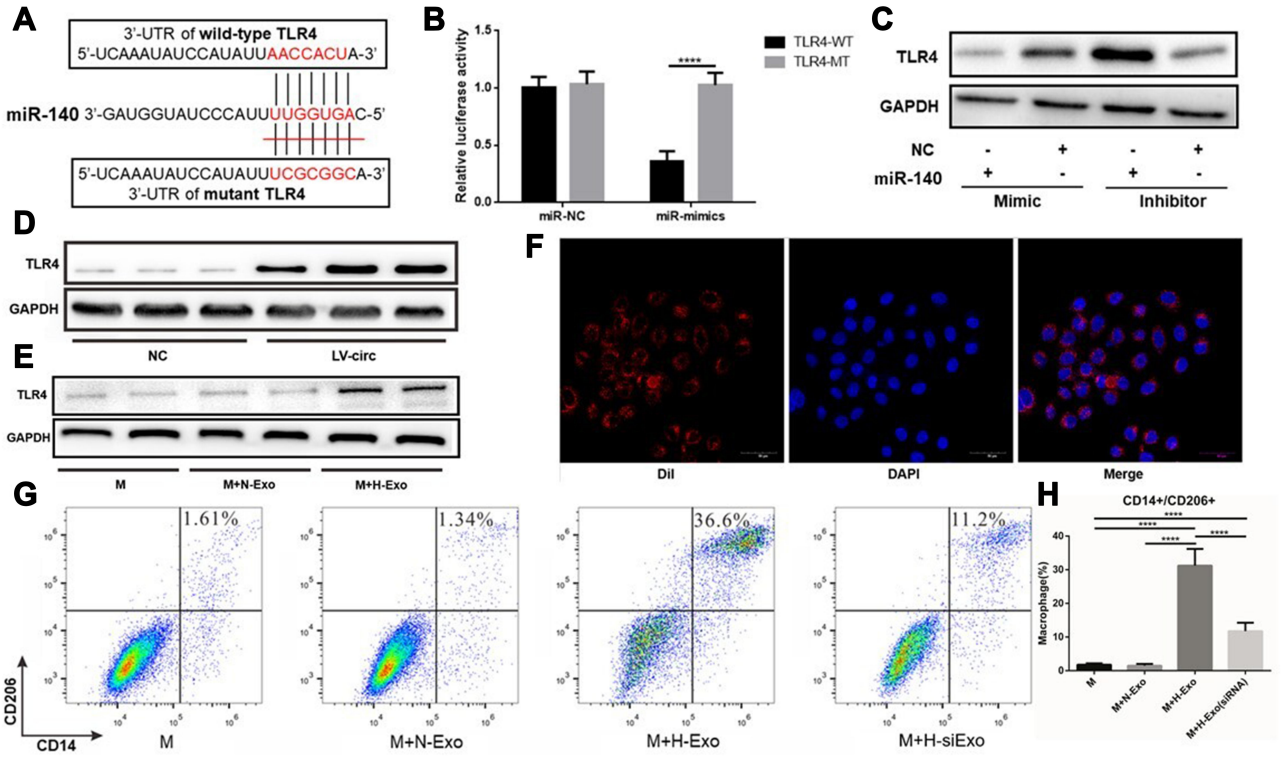

Figure 6 Exosomal hsa-circ-0048117 promotes M2 polarization by regulating miR-140-TLR4 axis. (**A**) The predicted binding site of 3′-UTR of TLR4 and miR-140. (**B**) The luciferase reporter experiment was applied to detect the luciferase activity after miR-140 mimics interacting with wild type TLR4 (****$p<0.001$). (**C**) Western blot was used to examine the TLR4 expression after miR-140 was upregulated and downregulated in macrophages. (**D**) The protein expression of TLR4 after hsa-circ-0048117 was overexpressed in macrophages. (**E**) The protein expression of TLR4 in macrophages co-cultured with exosomes derived from tumor cells under hypoxia or normoxia treatment. (**F**) The exosomes were isolated and dyed with DIL live cell tracer to observe their entry into macrophages. (**G** and **H**) Flow cytometry was used to detect the expression of M2 markers CD14 and CD206 after co-cultured with exosomes derived from tumor cells under normoxia and hypoxia (with or without hsa-circ-0048117 silenced) treatment (****$p<0.001$).

Abbreviations: M, macrophage; M+N-Exo, macrophage + normoxic-exosomes; M+H-Exo, macrophage + hypoxic-exosomes; M+H-siExo, macrophage + hypoxic-exosomes (circRNA-silenced).

Exosomal Hsa-Circ-0048117 Promotes M2 Macrophage Polarization and Invasion and Metastasis of ESCC

The exosomes were isolated and dyed with DIL live cell tracer to observe their entry into macrophages (Figure 6F). After co-culture with exosomes, macrophages were detected by flow cytometry and the results suggested the percentage of macrophages carrying both CD14 and CD206 was significantly increased after treatment of hypoxic exosomes ($p<0.01$) (Figure 6G and H). It was also found that TLR4 in macrophages was upregulated after co-culture with exosomes by hypoxic tumor cells according to the Western blot (Figure 6E). However, when hsa-circ-0048117 in tumor cells interfered with siRNA, the corresponding exosomes did not show a M2 macrophage polarization promotion after co-culture, the proportion of $CD14^+/CD206^+$ macrophages decreased significantly ($p<0.01$) (Figure 6G and H), suggesting hypoxia contributed to the synthesis of hsa-circ-0048117 which was packaged in exosomes and then secreted, after phagocytosed by macrophages, the highly expressed hsa-circ -0048117 promotes M2 macrophage polarization by upregulating TLR4.

After the establishment of a co-culture system including tumor cells, macrophages and exosomes (Figure 7A). Transwell invasion and migration experiments confirmed the number of tumor cells transported to the reverse side of the membrane increased when the macrophages in the lower chamber were treated with hypoxic exosomes compared to the 3 other groups ($p<0.01$) (Figure 7B-F and Figure S1 A-D), indicating that macrophages co-cultured with exosomes from hypoxia-stimulated tumor cells could enhance the invasion and migration ability of tumor cells (Eca-109 and TE-1). This promotion effect could be counteracted when hsa-circ-0048117 was silenced in the producer tumor cells. The expression of Arg1, IL-10 and TGF-β in the lower chamber medium was detected by ELISA. It was found that Arg1, IL-10 and TGF-β which are mainly secreted by M2 macrophages were significantly increased after co-culture with hypoxic exosomes ($p<0.01$) (Figure 7G-I), which further confirmed the M2 polarization promotive effect.

Comparing the expression of hsa-circ-0048117 in the exosomes from the serum of tumor patients and healthy volunteers, it was found that the expression of hsa-circ -0048117 in the serum exosomes of tumor patients was significantly higher than that in the healthy volunteers ($p<0.01$) (Figure 7D), and that exosomal hsa-circ -0048117 was positively related with T stage ($p = 0.018$), N stage ($p = 0.012$), and TNM grade ($p = 0.04$) of ESCC patients (Table 3).

Discussion

Hypoxia is an important part of the tumor microenvironment and regulates the biological function of a variety of tumor cells by modulating tumor immunity, releasing cytokines, and affecting tumor angiogenesis.[31] Solid tumors can cause local hypoxia due to the rapid proliferation of tumor cells. Hypoxic regions are usually located 100–150 um away from functional blood vessels. The oxygen pressure of normal human organs and tissues is 20–25 mmHg. Due to the growth of tumor tissues, lack of blood leads to oxygen pressure to be lower than 2.5 mmHg in most tumor tissues.[32,33] Hypoxia is closely related to the degree of tumor differentiation, lymph node metastasis, distant metastasis, and tumor tolerance to radiotherapy and chemotherapy.[34] Tumor-associated macrophages specifically refer to macrophages infiltrating around tumor tissues, which can secrete a variety of cytokines according to their polarity, and play an important role in tumorigenesis, invasion and metastasis.[35,36] The polarization of macrophages in tumors is often affected by the degree of hypoxia.[37] The tumor body is often in a state of hypoxia and high lactic acid stack, which leads to tumor blood vessels damage and tissue edema, resulting in an inflammatory response including accumulation of macrophages.[38] Previous studies found M2 macrophages were more common in ESCC tissues than in normal adjacent tissues. The degree of infiltration of M2 macrophages is statistically related to the prognosis, lymph node metastasis, and tumor invasion. M2 macrophages can promote epithelial-mesenchymal transition of ESCC cells and enhance the invasion and migration ability of ESCC cells.[39]

Tumor-derived exosomes contain a variety of functional molecules which could interact with the tumor microenvironment and establish an immunosuppressive environment that promotes tumor progression, thereby promoting tumor cell proliferation, anti-apoptosis, invasion and migration.[40,41] It has been found in glioblastoma, gastric cancer and pancreatic cancer that hypoxia can stimulate tumor cells to secrete more exosomes.[10,42,43] In pancreatic cancer, tumor cells generate miR-301a-3p-rich exosomes in a hypoxic microenvironment, which then polarize macrophages to promote malignant behaviors of PC cells.[10] Circular RNAs can be used as a competitive

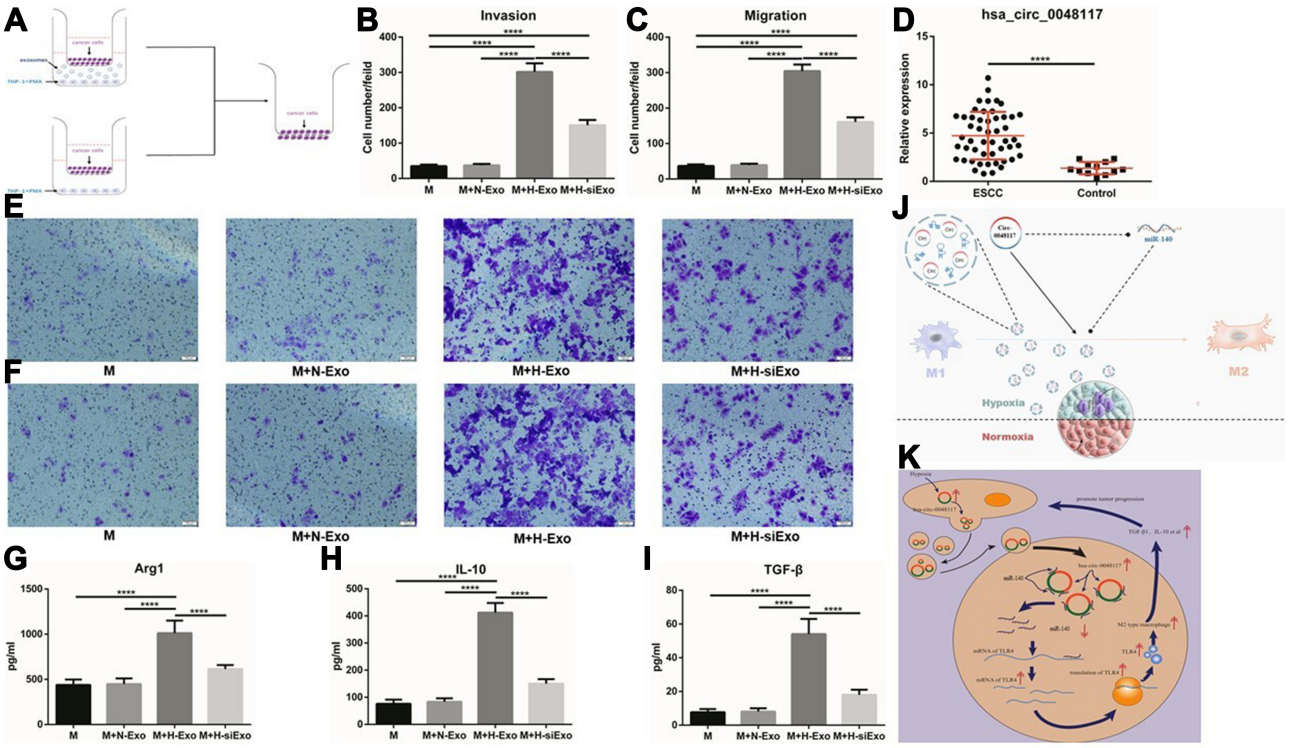

Figure 7 M2 macrophages could enhance the invasion and migration ability of ESCC cells. (**A**) Schematic illustration of the in vitro indirect co-culture system. (**B** and **E**) Invasion ability of Eca-109 cells co-cultured with macrophages treated with exosomes was determined by the in vitro transwell co-culture system (****p<0.001). (**C** and **F**) Migration ability of Eca-109 cells co-cultured with macrophages treated with exosomes was determined by the in vitro transwell co-culture system (****p<0.001). (**D**) The relative expression of exosomal hsa-circ-0048117 from serum of 50 ESCC patients and 12 healthy volunteers (****p<0.001). (**G–I**) The relative expression of Arg1, IL-10 and TGF-β in supernatants of macrophages co-cultured with exosomes derived from tumor cells under normoxia and hypoxia (with or without hsa-circ-0048117 silenced) treatment (****p<0.001). (**J**) The sketch illustration of our study. (**K**) The diagrammatic sketch of the molecular mechanism about our study.

Abbreviations: M, macrophage; M+N-Exo, macrophage + normoxic-exosomes; M+H-Exo, macrophage + hypoxic-exosomes; M+H-siExo, macrophage + hypoxic-exosomes (circRNA-silenced).

endogenous RNA by specifically adsorbing miRNAs.[19] Through high-throughput sequencing combined with bioinformatics analysis, we have discovered many differentially expressed circular RNAs and they may take part in the oncogenesis and progression of esophageal squamous cell carcinoma.[20–22] Studies have found that the abundance of circular RNA in tumor cell derived exosomes is higher than that in producer cells.[23] cir-ITCH targets miR-7, miR-17 and miR-214, enhancing the expression of ITCH, thereby inhibiting the proliferation of ESCC cells by inactivating the Wnt/β-catenin signaling pathway.[44] The expression of ciRS-7 was found upregulated in various ESCC cell lines and tumor tissues. High expression of ciRS-7 could enable tumor cells to dissolve stroma by secreting MMP2 and MMP9 and to migrate to other sites with blood flow.[45] ciRS-7 contains over 70 miR-7 binding sites, which can significantly inhibit the expression of miR-7 in ESCC and reverse upregulate the expression of EGFR, RAF1, PARP, SP1, PI3K by activating NF-κB.[46] A previous study found 189 differentially expressed circular RNAs between M1 and M2 macrophages,[47] some circular RNAs in glioma, breast cancer, and melanoma can promote the transformation of TAMs to M2 type,[41] but the relationship between circular RNAs and macrophages polarization has not been reported till date.

Our study found that hypoxic exosomal hsa-circ-0048117 could promote M2 polarization by competing to bind miR-140 with TLR4, and enhance the invasion and migration ability of tumor cells to promote the metastasis of ESCC (Figure 7K). However, there are some limitations about our study, we were not able to test our theory in vivo and the correlation between exosomal hsa-circ-0048117 and the prognosis has not been discussed, we will make our work complete in a further study.

Conclusion

In this study, we preliminarily investigated the comprehensive effect of hypoxia, exosomes, and circular RNA in the development of ESCC. We identified differentially expressed circular RNAs in exosomes secreted by tumor

Table 3 Correlation Between Serum Exo-Hsa-Circ0048117 and Clinicopathological Features

Features	Total	Hsa-circ-0048117	χ2	p
		Normal Up		
Age			0.005	0.941
≤60	18	3 15		
>60	32	7 25		
Gender			0.01	0.109
Male	43	8 35		
Female	7	2 5		
Tumor Location			0.006	0.941
Upper-middle 1/3	33	6 27		
Lower 1/3	17	4 13		
Differentiation			4.425	0.919
Well	5	3 2		
Moderate	33	5 28		
Poor	12	2 10		
Invasion			5.588	0.018*
T1-T2	21	8 13		
T3-T4	29	2 27		
Lymph node status			6.256	0.012*
Negative	16	7 9		
Positive	34	3 31		
TNM grade			4.232	0.040*
I-II	23	8 15		
III-IV	27	2 25		

Note: *P<0.05.

cells after hypoxia treatment. As a result, exosomal hsa-circ-0048117 was found to be capable of inducing TAMs differentiating to M2 type. Bioinformatic analysis, molecular biology and cell functions experiments confirmed that hsa-circ-0048117 can be used as a miR-140 "sponge" in macrophages (Figure 7J), and competes with TLR4 to bind miR-140, and hsa-circ-0048117 can upregulate TLR4 expression to promote M2 polarization. M2 macrophages could secrete Arg1, IL-10 and TGF-β which then enhance the invasion and migration ability of tumor cells, and promote the metastasis of ESCC. Serum exosomal hsa-circ-0048117 in ESCC patients was significantly higher than that in healthy volunteers. Higher exosomal hsa-circ -0048117 predicted an advanced T and N stage and was positively correlated with the TNM grade. Above all, our study demonstrated that exosomal hsa-circ-0048117 has the potential to serve as a new marker for the diagnosis and prognosis of ESCC patients.

Abbreviations

ESCC, esophageal squamous cell carcinoma; TAMs, tumor-associated macrophages; TEM, transmission electron microscopy; NTA, nanoparticle tracking analysis; TLR4, toll-like receptor 4; DMEM, Dulbecco's modified Eagle's medium; FBS, fetal bovine serum; PMA, phorbol-12-myristate-13-acetate.

Data Sharing Statement

All data generated or analyzed during this study are included in this published article.

Ethics Approval and Consent to Participate

The serum samples of patients were obtained with informed consent according to an established protocol approved by the Ethics Committee of Changhai Hospital.

Consent for Publication

All the patients that were involved in the study have given their consent to publish their individual data.

Author Contributions

All authors made substantial contributions to conception and design, acquisition of data, or analysis and interpretation of data; took part in drafting the article or revising it critically for important intellectual content; agreed to submit to the current journal; gave final approval of the version to be published; and agree to be accountable for all aspects of the work.

Funding

Our study was funded by Natural Science Foundation of Shanghai.

Disclosure

The authors report no conflicts of interest for this work.

References

1. Chen F, Zhuang X, Lin L, et al. New horizons in tumor microenvironment biology: challenges and opportunities. *BMC Med*. 2015;13:45. doi:10.1186/s12916-015-0278-7
2. Kaiko GE, Horvat JC, Beagley KW, et al. Immunological decision-making: how does the immune system decide to mount a helper T-cell response? *Immunology*. 2008;123:326–338. doi:10.1111/j.1365-2567.2007.02719.x
3. Akiyama K, Ohga N, Hida Y, et al. Tumor endothelial cells acquire drug resistance by MDR1 up-regulation via VEGF signaling in tumor microenvironment. *Am J Pathol*. 2012;180:1283–1293. doi:10.1016/j.ajpath.2011.11.029

4. Blansfield JA, Caragacianu D, Alexander HR, et al. Combining agents that target the tumor microenvironment improves the efficacy of anticancer therapy. *Clin Cancer Res*. 2008;14:270–280. doi:10.1158/1078-0432.CCR-07-1562
5. Finger EC, Giaccia AJ. Hypoxia, inflammation, and the tumor microenvironment in metastatic disease. *Cancer Metastasis Rev*. 2010;29:285–293. doi:10.1007/s10555-010-9224-5
6. Semenza GL. Oxygen sensing, hypoxia-inducible factors and disease pathophysiology. *Annu Rev Pathol*. 2014;9:47–71. doi:10.1146/annurev-pathol-012513-104720
7. Binker MG, Binker-Cosen AA, Richards D, et al. Hypoxia reoxygenation increase invasiveness of PANC-1 cells through Rac1/MMP-2. *Biochem Biophys Res Commun*. 2010;393:371–376. doi:10.1016/j.bbrc.2010.01.125
8. Rashed MH, Kanlikilicer P, Rodriguez-Aguayo C, et al. Exosomal miR-940 maintains SRC-mediated oncogenic activity in cancer cells: a possible role for exosomal disposal of tumor suppressor miRNAs. *Oncotarget*. 2017;8(12):20145–20164. doi:10.18632/oncotarget.15525
9. Shinohara H, Kuranaga Y, Kumazaki M, et al. Regulated polarization of tumor-associated macrophages by miR-145 via colorectal cancer-derived extracellular vesicles. *J Immunol*. 2017;199(4):1505–1515. doi:10.4049/jimmunol.1700167
10. Wang X, Luo G, Zhang K, et al. Hypoxic tumor-derived exosomal miR-301a Mediates M2 macrophage polarization via PTEN/PI3Kγ to promote pancreatic cancer metastasis. *Cancer Res*. 2018;78:16. doi:10.1158/0008-5472.CAN-17-3841
11. van der Pol E, Boing AN, Harrison P, et al. Classification, functions, and clinical relevance of extracellular vesicles. *Pharmacol Rev*. 2012;64:676–705.
12. Raposo G, Stoorvogel W. Extracellular vesicles: exosomes, microvesicles, and friends. *J Cell Biol*. 2013;200:373–383. doi:10.1083/jcb.201211138
13. Rodrigues G, Zhang H, Lyden D. Tumour vesicular micromachinery uncovered. *Nat Cell Biol*. 2019;21:795–797. doi:10.1038/s41556-019-0351-0
14. Whiteside TL. The emerging role of plasma exosomes in diagnosis, prognosis and therapies of patients with cancer. *Contemp Oncol*. 2018;22:38–40.
15. Azmi AS, Bao B, Sarkar FH. Exosomes in cancer development, metastasis, and drug resistance: a comprehensive review. *Cancer Metastasis Rev*. 2013;32:623–642.
16. Teng Y, Ren Y, Hu X, et al. MVP-mediated exosomal sorting of miR-193a promotes colon cancer progression. *Nat Commun*. 2017;8:14448. doi:10.1038/ncomms14448
17. Jeck WR, Sharpless NE. Detecting and characterizing circular RNAs. *Nat Biotechnol*. 2014;32(5):453–461. doi:10.1038/nbt.2890
18. Ashwal FR, Meyer M, Pamudurti NR, et al. circRNA biogenesis competes with pre-mRNA splicing. *Mol Cell*. 2014;56(1):55–66. doi:10.1016/j.molcel.2014.08.019
19. Li Z, Huang C, Bao C, et al. Exon-intron circular RNAs regulate transcription in the nucleus. *Nat Struct Mol Biol*. 2015;22(3):256–264. doi:10.1038/nsmb.2959
20. Wang F, Nazarali AJ, Circular JS. RNAs as potential biomarkers for cancer diagnosis and therapy. *Am J Cancer Res*. 2016;6:1167–1176.
21. Guarnerio J, Bezzi M, Jeong JC, et al. Oncogenic role of fusion-circRNAs derived from cancer-associated chromosomal translocations. *Cell*. 2016;165:289–302. doi:10.1016/j.cell.2016.03.020
22. Li P, Chen S, Chen H, et al. Using circular RNA as a novel type of biomarker in the screening of gastric cancer. *Clin Chim Acta*. 2015;444:132–136. doi:10.1016/j.cca.2015.02.018
23. Li Y, Zheng Q, Bao C, et al. Circular RNA is enriched and stable in exosomes: a promising biomarker for cancer diagnosis. *Cell Res*. 2015;25:981–984. doi:10.1038/cr.2015.82
24. Ratliff ML, Garton J, Garman L, et al. ARID3a gene profiles are strongly associated with human interferon alpha production. *J Autoimmun*. 2019;96:158–167. doi:10.1016/j.jaut.2018.09.013
25. Zhang Y, Xu Y, Li Z. Identification of the key transcription factors in esophageal squamous cell carcinoma. *J Thorac Dis*. 2018;10(1):148–161. doi:10.21037/jtd.2017.12.27
26. Ma J, Zhan Y, Xu Z, et al. ZEB1 induced miR-99b/let-7e/miR-125a cluster promotes invasion and metastasis in esophageal squamous cell carcinoma. *Cancer Lett*. 2017;398:37–45. doi:10.1016/j.canlet.2017.04.006
27. Chen T, Li Q, Wu J, et al. Fusobacterium nucleatum promotes M2 polarization of macrophages in the microenvironment of colorectal tumours via a TLR4-dependent mechanism. *Cancer Immunol Immunother*. 2018;67(10):204–215. doi:10.1007/s00262-018-2233-x
28. Oblak A, Jerala R. Toll-like receptor 4 activation in cancer progression and therapy. *Clin Dev Immunol*. 2011;2011:609579. doi:10.1155/2011/609579
29. Kawai T, Akira S. The role of pattern-recognition receptors in innate immunity: update on Toll-like receptors. *Nat Immunol*. 2010;11:373–384. doi:10.1038/ni.1863
30. Liu WT, Jing YY, Wei LX, et al. Toll like receptor 4 facilitates invasion and migration as a cancer stem cell marker in hepatocellular carcinoma. *Cancer Lett*. 2015;358:136–143. doi:10.1016/j.canlet.2014.12.019
31. Palazon A, Aragones J, Morales-Kastresana A, et al. Molecular pathways: hypoxia response in immune cells fighting or promoting cancer. *Clin Cancer Res*. 2012;18:1207–1213.
32. Palazon A, Aragones J, Morales-Kastresana A, et al. Molecular pathways: hypoxia response in immune cells fighting or promoting cancer. *Clin Cancer Res*. 2012;18:1207–1213. doi:10.1158/1078-0432.CCR-11-1591
33. Ratcliffe PJ. Oxygen sensing and hypoxia signalling pathways in animals: the implications of physiology for cancer. *J Physiol*. 2013;591(8):2027–2042. doi:10.1113/jphysiol.2013.251470
34. Lin A, Hahn SM. Hypoxia imaging markers and applications for radiation treatment planning. *Semin Nucl Med*. 2012;42:343–352. doi:10.1053/j.semnuclmed.2012.04.002
35. Allavena P, Mantovani A. Immunology in the clinic review series focus on cancer: tumour-associated macrophages: undisputed stars of the inflammatory tumour microenvironment. *Clin Exp Immunol*. 2012;167:195–205.
36. Qian BZ, Pollard JW. Macrophage diversity enhances tumor progression and metastasis. *Cell*. 2010;141:39–51. doi:10.1016/j.cell.2010.03.014
37. Staples KJ, Sotoode F, Pearson H, et al. Monocyte-derived macrophages matured under prolonged hypoxia transcriptionally up-regulate HIF-1alpha mRNA. *Immunobiology*. 2011;216(7):832–839. doi:10.1016/j.imbio.2010.12.005
38. Roda JM, Sumner LA, Evans R, et al. Hypoxia-inducible factor-2alpha regulates GM-CSF-derived soluble vascular endothelial growth factor receptor 1 production from macrophages and inhibits tumor growth and angiogenesis. *J Immunol*. 2011;187:1970–1976. doi:10.4049/jimmunol.1100841
39. Takase N, Koma Y-I, Urakawa N, et al. NCAM and FGF-2-mediated FGFR1 signaling in the tumor microenvironment of esophageal cancer regulates the survival and migration of tumor-associated macrophages and cancer cells. *Cancer Lett*. 2016;380:47–58. doi:10.1016/j.canlet.2016.06.009
40. Vaksman O, Trope C, Davidson B, et al. Exosome-derived miRNAs and ovarian carcinoma progression. *Carcinogenesis*. 2014;35:2113–2120. doi:10.1093/carcin/bgu130
41. Thakur BK, Zhang H, Becker A, et al. Double-stranded DNA in exosomes: a novel biomarker in cancer detection. *Cell Res*. 2014;24(6):766–769. doi:10.1038/cr.2014.44
42. Skog J, Würdinger T, van Rijn S, et al. Glioblastoma microvesicles transport RNA and proteins that promote tumour growth and provide diagnostic biomarkers. *Nat Cell Biol*. 2008;10(12):1470–1476. doi:10.1038/ncb1800
43. Qu JL, Qu XJ, Zhao MF, et al. Gastric cancer exosomes promote tumour cell proliferation through PI3K/Akt and MAPK/ERK activation. *Dig Liver Dis*. 2009;41(12):875–880. doi:10.1016/j.dld.2009.04.006

44. Li F, Zhang L, Li W, et al. Circular RNA ITCH has inhibitory effect on ESCC by suppressing the Wnt/beta-catenin pathway. *Oncotarget*. 2015;6:6001–6013. doi:10.18632/oncotarget.3469
45. Huang H, Wei L, Qin T, et al. Circular RNA ciRS-7 triggers the migration and invasion of esophageal squamous cell carcinoma via miR-7/KLF4 and NF-κB signals. *Cancer Biol Ther*. 2019;20 (1):73–80. doi:10.1080/15384047.2018.1507254
46. Li RC, Ke S, Meng FK, et al. CiRS-7 promotes growth and metastasis of esophageal squamous cell carcinoma via regulation of miR-7/HOXB13. *Cell Death Dis*. 2018;9(8):838. doi:10.1038/s41419-018-0852-y
47. Zhang Y, Zhang Y, Li X, et al. Microarray analysis of circular RNA expression patterns in polarized macrophages. *Int J Mol Med*. 2017;39(2):373–379. doi:10.3892/ijmm.2017.2852